

Observation of Diffractively Produced W and Z Bosons in $\bar{p}p$ Collisions at $\sqrt{s} = 1800$ GeV

V.M. Abazov,²¹ B. Abbott,⁵⁵ A. Abdesselam,¹¹ M. Abolins,⁴⁸ V. Abramov,²⁴ B.S. Acharya,¹⁷
D.L. Adams,⁵³ M. Adams,³⁵ S.N. Ahmed,²⁰ G.D. Alexeev,²¹ A. Alton,⁴⁷ G.A. Alves,²
E.W. Anderson,⁴⁰ Y. Arnoud,⁹ C. Avila,⁵ V.V. Babintsev,²⁴ L. Babukhadia,⁵² T.C. Bacon,²⁶
A. Baden,⁴⁴ S. Baffioni,¹⁰ B. Baldin,³⁴ P.W. Balm,¹⁹ S. Banerjee,¹⁷ E. Barberis,⁴⁶ P. Baringer,⁴¹
J. Barreto,² J.F. Bartlett,³⁴ U. Bassler,¹² D. Bauer,³⁸ A. Bean,⁴¹ F. Beaudette,¹¹ M. Begel,⁵¹
A. Belyaev,³³ S.B. Beri,¹⁵ G. Bernardi,¹² I. Bertram,²⁵ A. Besson,⁹ R. Beuselinck,²⁶
V.A. Bezzubov,²⁴ P.C. Bhat,³⁴ V. Bhatnagar,¹⁵ M. Bhattacharjee,⁵² G. Blazey,³⁶ F. Blekman,¹⁹
S. Blessing,³³ A. Boehnlein,³⁴ N.I. Bojko,²⁴ T.A. Bolton,⁴² F. Borcharding,³⁴ K. Bos,¹⁹ T. Bose,⁵⁰
A. Brandt,⁵⁷ G. Briskin,⁵⁶ R. Brock,⁴⁸ G. Brooijmans,³⁴ A. Bross,³⁴ D. Buchholz,³⁷ M. Buehler,³⁵
V. Buescher,¹⁴ V.S. Burtovoi,²⁴ J.M. Butler,⁴⁵ F. Canelli,⁵¹ W. Carvalho,³ D. Casey,⁴⁸
H. Castilla-Valdez,¹⁸ D. Chakraborty,³⁶ K.M. Chan,⁵¹ S.V. Chekulaev,²⁴ D.K. Cho,⁵¹ S. Choi,³²
S. Chopra,⁵³ D. Claes,⁴⁹ A.R. Clark,²⁸ L. Coney,⁵⁰ B. Connolly,³³ W.E. Cooper,³⁴ D. Coppage,⁴¹
S. Crépé-Renaudin,⁹ M.A.C. Cummings,³⁶ D. Cutts,⁵⁶ H. da Motta,² G.A. Davis,⁵¹ K. De,⁵⁷
S.J. de Jong,²⁰ M. Demarteau,³⁴ R. Demina,⁵¹ P. Demine,¹³ D. Denisov,³⁴ S.P. Denisov,²⁴
S. Desai,⁵² H.T. Diehl,³⁴ M. Diesburg,³⁴ S. Doulas,⁴⁶ L.V. Dudko,²³ S. Duensing,²⁰ L. Dufлот,¹¹
S.R. Dugad,¹⁷ A. Duperrin,¹⁰ A. Dyshkant,³⁶ D. Edmunds,⁴⁸ J. Ellison,³² J.T. Eltzroth,⁵⁷
V.D. Elvira,³⁴ R. Engelmann,⁵² S. Eno,⁴⁴ G. Eppley,⁵⁸ P. Ermolov,²³ O.V. Eroshin,²⁴
J. Estrada,⁵¹ H. Evans,⁵⁰ V.N. Evdokimov,²⁴ D. Fein,²⁷ T. Ferbel,⁵¹ F. Filthaut,²⁰ H.E. Fisk,³⁴
F. Fleuret,¹² M. Fortner,³⁶ H. Fox,³⁷ S. Fu,⁵⁰ S. Fuess,³⁴ E. Gallas,³⁴ A.N. Galyaev,²⁴ M. Gao,⁵⁰
V. Gavrilo, ²² R.J. Genik II,²⁵ K. Genser,³⁴ C.E. Gerber,³⁵ Y. Gershtein,⁵⁶ G. Ginther,⁵¹
B. Gómez,⁵ P.I. Goncharov,²⁴ H. Gordon,⁵³ K. Gounder,³⁴ A. Goussiou,²⁶ N. Graf,⁵³
P.D. Grannis,⁵² J.A. Green,⁴⁰ H. Greenlee,³⁴ Z.D. Greenwood,⁴³ S. Grinstein,¹ L. Groer,⁵⁰
S. Grünendahl,³⁴ S.N. Gurzhiev,²⁴ G. Gutierrez,³⁴ P. Gutierrez,⁵⁵ N.J. Hadley,⁴⁴ H. Haggerty,³⁴
S. Hagopian,³³ V. Hagopian,³³ R.E. Hall,³⁰ C. Han,⁴⁷ S. Hansen,³⁴ J.M. Hauptman,⁴⁰
C. Hebert,⁴¹ D. Hedin,³⁶ J.M. Heinmiller,³⁵ A.P. Heinson,³² U. Heintz,⁴⁵ M.D. Hildreth,³⁹
R. Hirosky,⁵⁹ J.D. Hobbs,⁵² B. Hoeneisen,⁸ J. Huang,³⁸ Y. Huang,⁴⁷ I. Iashvili,³² R. Illingworth,²⁶
A.S. Ito,³⁴ M. Jaffré,¹¹ S. Jain,¹⁷ R. Jesik,²⁶ K. Johns,²⁷ M. Johnson,³⁴ A. Jonckheere,³⁴
H. Jöstlein,³⁴ A. Juste,³⁴ W. Kahl,⁴² S. Kahn,⁵³ E. Kajfasz,¹⁰ A.M. Kalinin,²¹ D. Karmanov,²³
D. Karmgard,³⁹ R. Kehoe,⁴⁸ A. Khanov,⁵¹ A. Kharchilava,³⁹ B. Klima,³⁴ J.M. Kohli,¹⁵
A.V. Kostritskiy,²⁴ J. Kotcher,⁵³ B. Kothari,⁵⁰ A.V. Kozelov,²⁴ E.A. Kozlovsky,²⁴ J. Krane,⁴⁰
M.R. Krishnaswamy,¹⁷ P. Krivkova,⁶ S. Krzywdzinski,³⁴ M. Kubantsev,⁴² S. Kuleshov,²²
Y. Kulik,³⁴ S. Kunori,⁴⁴ A. Kupco,⁷ V.E. Kuznetsov,³² G. Landsberg,⁵⁶ W.M. Lee,³³ A. Leflat,²³
F. Lehner,^{34,*} C. Leonidopoulos,⁵⁰ J. Li,⁵⁷ Q.Z. Li,³⁴ J.G.R. Lima,³ D. Lincoln,³⁴ S.L. Linn,³³
J. Linnemann,⁴⁸ R. Lipton,³⁴ A. Lucotte,⁹ L. Lueking,³⁴ C. Lundstedt,⁴⁹ C. Luo,³⁸
A.K.A. Maciel,³⁶ R.J. Madaras,²⁸ V.L. Malyshev,²¹ V. Manankov,²³ H.S. Mao,⁴ T. Marshall,³⁸
M.I. Martin,³⁶ K. Mauritz,⁴⁰ A.A. Mayorov,²⁴ R. McCarthy,⁵² T. McMahon,⁵⁴ H.L. Melanson,³⁴
M. Merkin,²³ K.W. Merritt,³⁴ C. Miao,⁵⁶ H. Miettinen,⁵⁸ D. Mihalcea,³⁶ N. Mokhov,³⁴
N.K. Mondal,¹⁷ H.E. Montgomery,³⁴ R.W. Moore,⁴⁸ Y.D. Mutaf,⁵² E. Nagy,¹⁰ F. Nang,²⁷

M. Narain,⁴⁵ V.S. Narasimham,¹⁷ N.A. Naumann,²⁰ H.A. Neal,⁴⁷ J.P. Negret,⁵ A. Nomerotski,³⁴
T. Nunnemann,³⁴ D. O’Neil,⁴⁸ V. Oguri,³ B. Olivier,¹² N. Oshima,³⁴ P. Padley,⁵⁸
K. Papageorgiou,³⁵ N. Parashar,⁴³ R. Partridge,⁵⁶ N. Parua,⁵² A. Patwa,⁵² O. Peters,¹⁹
P. Pétroff,¹¹ R. Piegaia,¹ B.G. Pope,⁴⁸ H.B. Prosper,³³ S. Protopopescu,⁵³ M.B. Przybycien,^{37,†}
J. Qian,⁴⁷ R. Raja,³⁴ S. Rajagopalan,⁵³ P.A. Rapidis,³⁴ N.W. Reay,⁴² S. Reucroft,⁴⁶ M. Ridel,¹¹
M. Rijssenbeek,⁵² F. Rizatdinova,⁴² T. Rockwell,⁴⁸ C. Royon,¹³ P. Rubinov,³⁴ R. Ruchti,³⁹
B.M. Sabirov,²¹ G. Sajot,⁹ A. Santoro,³ L. Sawyer,⁴³ R.D. Schamberger,⁵² H. Schellman,³⁷
A. Schwartzman,¹ E. Shabalina,³⁵ R.K. Shivpuri,¹⁶ D. Shpakov,⁴⁶ M. Shupe,²⁷ R.A. Sidwell,⁴²
V. Simak,⁷ V. Sirotenko,³⁴ P. Slattery,⁵¹ R.P. Smith,³⁴ G.R. Snow,⁴⁹ J. Snow,⁵⁴ S. Snyder,⁵³
J. Solomon,³⁵ Y. Song,⁵⁷ V. Sorín,¹ M. Sosebee,⁵⁷ N. Sotnikova,²³ K. Soustruznik,⁶ M. Souza,²
N.R. Stanton,⁴² G. Steinbrück,⁵⁰ D. Stoker,³¹ V. Stolin,²² A. Stone,⁴³ D.A. Stoyanova,²⁴
M.A. Strang,⁵⁷ M. Strauss,⁵⁵ M. Strovink,²⁸ L. Stutte,³⁴ A. Sznajder,³ M. Talby,¹⁰ W. Taylor,⁵²
S. Tentindo-Repond,³³ S.M. Tripathi,²⁹ T.G. Trippe,²⁸ A.S. Turcot,⁵³ P.M. Tuts,⁵⁰
R. Van Kooten,³⁸ V. Vaniev,²⁴ N. Varelas,³⁵ F. Villeneuve-Seguer,¹⁰ A.A. Volkov,²⁴
A.P. Vorobiev,²⁴ H.D. Wahl,³³ Z.-M. Wang,⁵² J. Warchol,³⁹ G. Watts,⁶⁰ M. Wayne,³⁹ H. Weerts,⁴⁸
A. White,⁵⁷ D. Whiteson,²⁸ D.A. Wijngaarden,²⁰ S. Willis,³⁶ S.J. Wimpenny,³² J. Womersley,³⁴
D.R. Wood,⁴⁶ Q. Xu,⁴⁷ R. Yamada,³⁴ P. Yamin,⁵³ T. Yasuda,³⁴ Y.A. Yatsunenkov,²¹ K. Yip,⁵³
J. Yu,⁵⁷ M. Zanabria,⁵ X. Zhang,⁵⁵ H. Zheng,³⁹ B. Zhou,⁴⁷ Z. Zhou,⁴⁰ M. Zielinski,⁵¹
D. Zieminska,³⁸ A. Zieminski,³⁸ V. Zutshi,³⁶ E.G. Zverev,²³ and A. Zylberstejn¹³

(DØ Collaboration)

¹ *Universidad de Buenos Aires, Buenos Aires, Argentina*

² *LAFEX, Centro Brasileiro de Pesquisas Físicas, Rio de Janeiro, Brazil*

³ *Universidade do Estado do Rio de Janeiro, Rio de Janeiro, Brazil*

⁴ *Institute of High Energy Physics, Beijing, People’s Republic of China*

⁵ *Universidad de los Andes, Bogotá, Colombia*

⁶ *Charles University, Center for Particle Physics, Prague, Czech Republic*

⁷ *Institute of Physics, Academy of Sciences, Center for Particle Physics, Prague, Czech Republic*

⁸ *Universidad San Francisco de Quito, Quito, Ecuador*

⁹ *Laboratoire de Physique Subatomique et de Cosmologie, IN2P3-CNRS, Université de Grenoble 1, Grenoble, France*

¹⁰ *CPPM, IN2P3-CNRS, Université de la Méditerranée, Marseille, France*

¹¹ *Laboratoire de l’Accélérateur Linéaire, IN2P3-CNRS, Orsay, France*

¹² *LPNHE, Universités Paris VI and VII, IN2P3-CNRS, Paris, France*

¹³ *DAPNIA/Service de Physique des Particules, CEA, Saclay, France*

¹⁴ *Universität Mainz, Institut für Physik, Mainz, Germany*

¹⁵ *Panjab University, Chandigarh, India*

¹⁶ *Delhi University, Delhi, India*

¹⁷ *Tata Institute of Fundamental Research, Mumbai, India*

¹⁸ *CINVESTAV, Mexico City, Mexico*

¹⁹ *FOM-Institute NIKHEF and University of Amsterdam/NIKHEF, Amsterdam, The Netherlands*

²⁰ *University of Nijmegen/NIKHEF, Nijmegen, The Netherlands*

²¹ *Joint Institute for Nuclear Research, Dubna, Russia*

- ²²*Institute for Theoretical and Experimental Physics, Moscow, Russia*
- ²³*Moscow State University, Moscow, Russia*
- ²⁴*Institute for High Energy Physics, Protvino, Russia*
- ²⁵*Lancaster University, Lancaster, United Kingdom*
- ²⁶*Imperial College, London, United Kingdom*
- ²⁷*University of Arizona, Tucson, Arizona 85721*
- ²⁸*Lawrence Berkeley National Laboratory and University of California, Berkeley, California 94720*
- ²⁹*University of California, Davis, California 95616*
- ³⁰*California State University, Fresno, California 93740*
- ³¹*University of California, Irvine, California 92697*
- ³²*University of California, Riverside, California 92521*
- ³³*Florida State University, Tallahassee, Florida 32306*
- ³⁴*Fermi National Accelerator Laboratory, Batavia, Illinois 60510*
- ³⁵*University of Illinois at Chicago, Chicago, Illinois 60607*
- ³⁶*Northern Illinois University, DeKalb, Illinois 60115*
- ³⁷*Northwestern University, Evanston, Illinois 60208*
- ³⁸*Indiana University, Bloomington, Indiana 47405*
- ³⁹*University of Notre Dame, Notre Dame, Indiana 46556*
- ⁴⁰*Iowa State University, Ames, Iowa 50011*
- ⁴¹*University of Kansas, Lawrence, Kansas 66045*
- ⁴²*Kansas State University, Manhattan, Kansas 66506*
- ⁴³*Louisiana Tech University, Ruston, Louisiana 71272*
- ⁴⁴*University of Maryland, College Park, Maryland 20742*
- ⁴⁵*Boston University, Boston, Massachusetts 02215*
- ⁴⁶*Northeastern University, Boston, Massachusetts 02115*
- ⁴⁷*University of Michigan, Ann Arbor, Michigan 48109*
- ⁴⁸*Michigan State University, East Lansing, Michigan 48824*
- ⁴⁹*University of Nebraska, Lincoln, Nebraska 68588*
- ⁵⁰*Columbia University, New York, New York 10027*
- ⁵¹*University of Rochester, Rochester, New York 14627*
- ⁵²*State University of New York, Stony Brook, New York 11794*
- ⁵³*Brookhaven National Laboratory, Upton, New York 11973*
- ⁵⁴*Langston University, Langston, Oklahoma 73050*
- ⁵⁵*University of Oklahoma, Norman, Oklahoma 73019*
- ⁵⁶*Brown University, Providence, Rhode Island 02912*
- ⁵⁷*University of Texas, Arlington, Texas 76019*
- ⁵⁸*Rice University, Houston, Texas 77005*
- ⁵⁹*University of Virginia, Charlottesville, Virginia 22901*
- ⁶⁰*University of Washington, Seattle, Washington 98195*
- (February 7, 2008)

Abstract

Using the DØ detector, we have observed events produced in $\bar{p}p$ collisions that contain W or Z bosons in conjunction with very little energy deposition (“rapidity gaps”) in large forward regions of the detector. The fraction of W boson events with a rapidity gap (a signature for diffraction) is $0.89 \pm_{0.17}^{0.19} \%$, and the probability that the non-diffractive background fluctuated to yield the observed diffractive signal is 3×10^{-14} , corresponding to a significance of 7.5σ . The Z boson sample has a gap fraction of $1.44 \pm_{0.52}^{0.61} \%$, with a significance of 4.4σ . The diffractive events have very similar properties to the more common non-diffractive component.

Inelastic diffractive collisions are responsible for about 15% of the $\bar{p}p$ total cross section, and have been described by Regge theory through the exchange of a pomeron [1]. Such events are characterized by a proton (or antiproton) carrying away most of the beam momentum, and by the absence of significant hadronic particle activity over a large region of pseudorapidity ($\eta = -\ln[\tan(\frac{\theta}{2})]$, where θ is the polar angle relative to the beam). This empty region is called a rapidity gap and can be used as an experimental signature for diffraction. Ingelman and Schlein proposed the possibility of a partonic structure for the pomeron, which would lead to hard scattering in diffractive events [2]. This so-called “hard diffraction” was first observed by the UA8 experiment [3] at the CERN $S\bar{p}pS$ collider in the form of jet events with an associated tagged proton.

Initial rapidity-gap-based analyses of diffractive jet [4–6], b -quark [7], and J/Ψ [8] production are qualitatively consistent with a predominantly hard gluonic pomeron, but the production cross sections observed at the Fermilab Tevatron are far lower than predictions based on data from the DESY ep collider HERA [4,9]. Diffractive jet results from the CDF collaboration using an antiproton tag [10] confirm the normalization discrepancy between Tevatron ($\sqrt{s} = 1800$ GeV) and HERA data, while recent DØ rapidity-gap-based diffractive jet results at $\sqrt{s} = 1800$ GeV and $\sqrt{s} = 630$ GeV [11] show that a simple normalization difference cannot accommodate the Tevatron data (and imply that a significant soft gluon component is needed to “save” the Ingelman-Schlein model). A unified picture within this framework requires a detailed understanding of gap survival probability, which includes effects from multiple parton scattering and extra gluon emission associated with the hard sub-process [12]. The soft color interaction (SCI) model [13], which hypothesizes that non-perturbative gluon emissions can create rapidity gaps, provides an alternative description of diffraction without invoking pomeron dynamics, and predicts diffractive rates similar to those observed.

Bruni and Ingelman [14] proposed that a search for diffractive production of W and Z bosons would provide important information on diffractive structure, due to their sensitivity to quark sub-structure. They predicted that a pomeron composed primarily of quarks would lead to more than 15% of W and Z bosons being diffractively produced. The SCI model, on the other hand, predicts a diffractive fraction of about 1% [15].

The CDF collaboration observed a 3.8 standard deviation (σ) signal for diffractive W boson production, extracting the signal using the asymmetry of both lepton charge and position relative

to the region of the rapidity gap, and obtained a diffractive to non-diffractive production ratio of $(1.15 \pm 0.55)\%$ [16]. In this Letter, we present a definitive observation of diffractively produced W and Z bosons. We present characteristics of diffractive W bosons, and measurements of the fraction of W and Z boson events that contain forward rapidity gaps. In addition, we provide the ratio of diffractive W and Z cross sections, and the fraction of the initial momentum carried away by the scattered proton in the collision.

In the DØ detector [17], electrons are measured and missing transverse energy (\cancel{E}_T) determined using the uranium/liquid-argon calorimeters, with electromagnetic coverage to $|\eta| = 4.1$ and coverage for hadrons to $|\eta| = 5.2$. Electron identification, described in more detail below, requires a central or forward drift chamber track to match the location of the associated electromagnetic cluster. For the period during which the data were collected, the DØ detector had no magnetic field within the central tracking volume, consequently electrons and positrons could not be differentiated and are both referred to as electrons.

To identify rapidity gaps, we count the number of tiles containing a signal in the LØ forward scintillator arrays ($n_{\text{LØ}}$) and the number of calorimeter towers ($\Delta\eta \times \Delta\phi = 0.1 \times 0.1$) with signals above threshold (n_{CAL}). The LØ arrays provide partial coverage in the region $2.3 < |\eta| < 4.3$. A portion of the two forward calorimeters ($3.0 < |\eta| < 5.2$) is used to measure the calorimeter multiplicity, with a particle tagged by the deposition of more than 150 (500) MeV of energy in an electromagnetic (hadronic) tower. These thresholds are set to minimize noise from radioactive decays in the uranium, while maximizing sensitivity to energetic particles [18].

For this analysis, we search for the presence of rapidity gaps in inclusive samples of $W \rightarrow e\nu$ events and $Z \rightarrow e^+e^-$ events, based on data with an integrated luminosity of approximately 85 pb^{-1} accumulated during the 1994–1995 collider run (Run Ib). The DØ collaboration has extensively studied W and Z boson production in the electron channel [19,20]. The requirements for the event selection in this analysis are nearly identical to those of Ref. [20], with two notable exceptions detailed below. The data were obtained using a single hardware trigger that required at least one electromagnetic (EM) object with transverse energy (E_T) greater than 15 GeV, with more than 85% of its energy deposited in the EM section of the calorimeter (EM fraction). At the software trigger level, the EM cluster is required to satisfy isolation, shower-shape, and EM fraction criteria consistent with the presence of an electron. For the W boson sample, we require this candidate electron to have an $E_T > 20$ GeV, and additionally require $\cancel{E}_T > 15$ GeV for the neutrino, while for the Z boson sample, we require two electron candidates with $E_T > 16$ GeV.

The first significant difference between the data samples in this analysis and those of Ref. [20] is that we are unable to include events from the first portion of Run Ib, during which a coincidence (in the LØ detector) between the remnants of the proton and antiproton was required, effectively vetoing single-diffractive production. Restricting this analysis to the part of the data collected without this condition reduces the sample by 30%. The only other major difference is that this analysis requires the removal of events with more than one proton-antiproton interaction in the same bunch crossing. This “single interaction” requirement is necessary for rapidity-gap-based diffractive studies, because the presence of additional events obscures the rapidity-gap signature. About 70% of the remaining data sample is discarded as a result of this requirement, which makes use primarily of timing information in the luminosity counters and the number of vertices found

in the central tracker to reject multiple interaction events.

Variable	Comment	Events
Trigger	electron + \cancel{E}_T	119,890
No L \emptyset requirement in trigger		84,310
Main ring cuts		63,978
Single interaction		17,870
One electron in fiducial region	$ \eta < 1.1$ or $1.5 < \eta < 2.5$	17,626
E_T of electron	> 25 GeV	15,203
Electron quality	isolation, shape, EM fraction	13,770
\cancel{E}_T	> 25 GeV	12,622
Total $W \rightarrow e\nu$ sample		12,622
Central e sample	$ \eta < 1.1$	8,724
Forward e sample	$1.5 < \eta < 2.5$	3,898

TABLE I. Central and forward W boson event selection criteria.

The other analysis cuts are all standard criteria employed in D \emptyset electron analyses. In addition to a 25 GeV threshold on the event \cancel{E}_T and the electron E_T , and further selection based on the electron quality, events that occurred during the injection of proton bunches in the Main Ring accelerator are rejected (these often produced significant energy deposition in the D \emptyset calorimeter) [19]. The final data samples consist of 811 Z boson candidate events, and 12,622 W boson candidate events, of which 8,724 have a central electron ($|\eta| < 1.1$) and 3,898 have a forward electron ($1.5 < |\eta| < 2.5$). A summary of the event selections is given in Tables I and II.

Figure 1 shows two views of $n_{L\emptyset}$ versus n_{CAL} for the combined central and forward W boson sample. The multiplicity in the forward η interval with the lower n_{CAL} multiplicity (for some events this interval is at $+\eta$ and for others $-\eta$) is plotted for Fig. 1(a) and (b) for the full range of multiplicity and for the region of low multiplicity ($n_{CAL} < 20$, $n_{L\emptyset} < 10$), respectively. The distributions peak at zero multiplicity ($n_{CAL} = n_{L\emptyset} = 0$), in qualitative agreement with expectations for a diffractive component in the data. Figure 2 shows this scatter plot separately for the (a) central and (b) forward W boson samples, and for the (c) Z boson sample. All samples show clear evidence for a diffractive component at low multiplicity.

We now compare characteristics of the diffractive W boson candidates to the non-diffractive events to verify that these are typical W bosons, except for the presence of a rapidity gap. Figures 3(a), (c), and (e) show the electron E_T , \cancel{E}_T , and transverse mass (M_T), respectively, for standard W boson events ($n_{CAL} > 1$), while Figs. 3(b), (d), and (f) show the corresponding quantities for diffractive candidate events ($n_{L\emptyset} = n_{CAL} = 0$). Although the statistics in the diffractive sample are limited, the distributions in all three variables are very similar. The mean values for these quantities for the non-diffractive and diffractive samples, respectively, are in excellent agree-

Variable	Comment	Events
Trigger	two electrons	13,912
No L \emptyset requirement in trigger		10,023
Main ring cuts		8,751
Single interaction		2,381
Two electrons in fiducial region	$ \eta < 1.1$ or $1.5 < \eta < 2.5$	1,617
E_T of electrons	> 25 GeV	1,046
Electron quality	isolation, shape, EM fraction	893
Invariant mass window	$76 < M_{ee} < 106$ GeV/ c^2	811
Total $Z \rightarrow e^+e^-$ sample		811

TABLE II. Z boson event selection criteria.

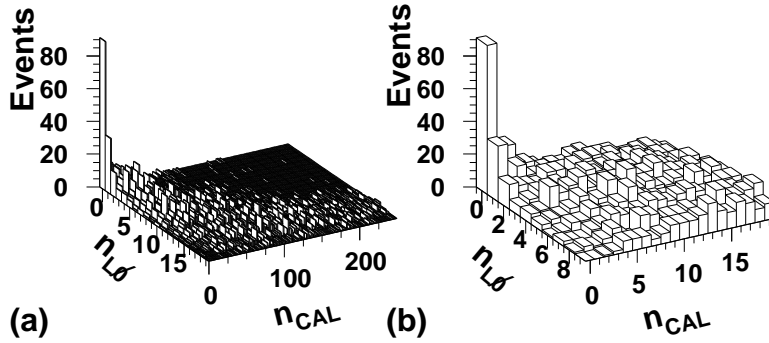


FIG. 1. The multiplicity in forward tiles ($n_{L\emptyset}$) and in calorimeter towers (n_{CAL}) for the forward region with the lower multiplicity, for the combined central and forward electron W boson samples: (a) shows the full range of multiplicity, (b) shows expanded region of low multiplicity ($n_{CAL} < 20$, $n_{L\emptyset} < 10$).

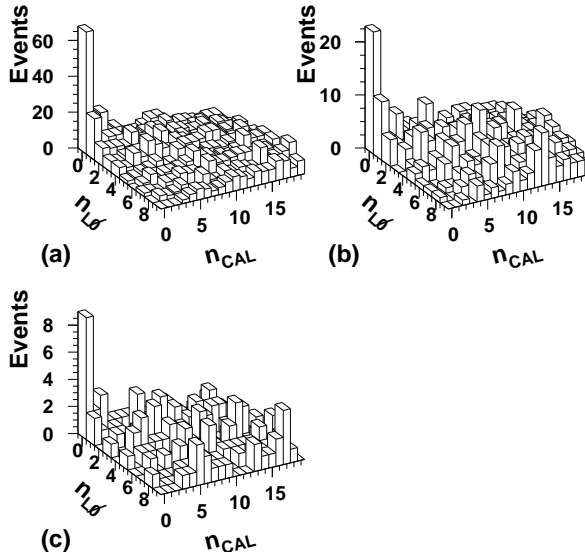


FIG. 2. The forward tile versus calorimeter tower multiplicity for (a) the central W boson sample, (b) the forward W boson sample, and (c) the Z boson sample.

ment: $\langle E_T \rangle = 35.2$ versus 35.1 GeV, $\langle \cancel{E}_T \rangle = 36.9$ versus 36.5 GeV, and $\langle M_T \rangle = 70.4$ versus 72.5 GeV/ c^2 , with uncertainties of about 3% on the latter values due to the limited statistics for diffractive candidates (91 events).

The fractions of W and Z boson events that contain forward rapidity gaps (“gap fraction”) are extracted from fits to the data in Fig. 2. The non-diffractive (high multiplicity) background in the signal region is represented by a four-parameter polynomial surface, and the signal by a two-dimensional falling exponential as in Ref. [11]. Figure 4 shows the multiplicity distribution from Fig. 2(a), and the resulting fitted signal, fitted background, and the normalized distribution of pulls ($[\text{data-fit}]/\sqrt{N}$). The $\chi^2/\text{dof} = 1.04$ for this fit, and all other fits are of comparable quality.

The fitting process is repeated over a systematically varied range of $n_{L\emptyset}$ (lower limit of 2 tiles and upper limit ranging from 5 to 7 tiles) and n_{CAL} (lower limit of 3 towers and upper limit ranging from 6 to 12 towers) to minimize any dependence of the signal on the chosen region. The result is a distribution of gap fractions, with the final signal defined by the mean of this distribution. The statistics in the Z boson sample are insufficient to perform an independent fit, so we use the background shape from the combined W boson sample scaled to the Z boson data to determine the diffractive Z boson signal. Varying the shape of the background samples used for the fit shows only small variations in the signal, well within the quoted uncertainties.

To determine the final gap fractions, we correct the fitted values for residual contamination from multiple interaction events which were not rejected by the single interaction requirement. These events contribute only to the denominator of the gap fraction, resulting in a measured gap fraction that is lower than the correct value. This correction is determined using the full data sample with no single interaction requirement by comparing the predicted number of single interaction events (based on the instantaneous luminosity) with the observed number of events after the single

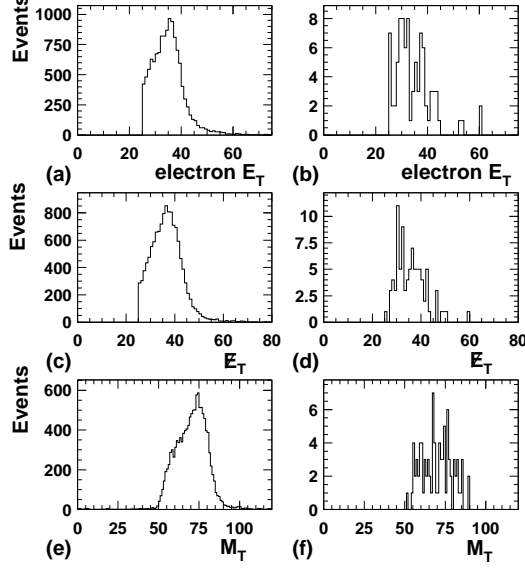


FIG. 3. Event characteristics for standard W boson events (left column, $n_{\text{CAL}} > 1$), compared to diffractive W boson candidates (right column, $n_{\text{CAL}} = n_{\text{LO}} = 0$). The top plots compare electron E_T , the middle plots show E_T , and the bottom plots compare the transverse mass (M_T) for the two cases.

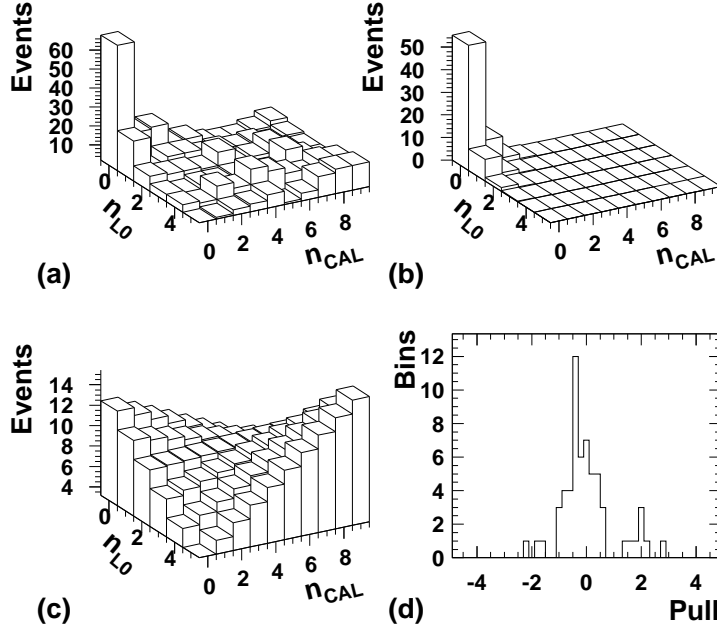


FIG. 4. The (a) n_{LO} versus n_{CAL} distribution for the central electron W boson data from Fig. 2(a), and corresponding (b) fitted signal, (c) fitted background, and (d) normalized pull distributions.

interaction selection. This method demonstrates that our single interaction requirement is quite effective, and yields only an absolute correction of $(0.09 \pm 0.05)\%$ for the central electron W boson and the Z boson samples and a negligible correction for the forward electron W boson sample.

Table III summarizes the final gap fractions obtained for the W and Z boson samples and their significances. The combined W boson sample has a gap fraction of $0.89 \pm_{0.17}^{0.19}\%$ and a probability that the non-diffractive background fluctuated to the diffractive signal of 3×10^{-14} , corresponding to a significance of 7.5σ . The central W boson fraction (electron $|\eta| < 1.1$) of $1.08 \pm_{0.17}^{0.19}\%$ is greater than the forward fraction ($1.5 < |\eta| < 2.5$) of $0.64 \pm_{0.16}^{0.18}\%$, unlike for jet events [11] (or typical diffractive expectations), which have a larger forward fraction. The Z boson sample has a gap fraction of $1.44 \pm_{0.52}^{0.61}\%$, with a significance of 4.4σ . Uncertainties are dominated by those on the fit parameters. Additional small uncertainties from the dependence on the range of multiplicities used in the fits are added in quadrature. Potential sources of systematic error, such as the number of fit parameters, electron quality criteria, tower thresholds, and residual noise, yield only negligible variations in the gap fractions [18,21].

Sample	Gap Fraction	Significance
Central $W \rightarrow e\nu$ ($ \eta < 1.1$)	$(1.08 + 0.19 - 0.17)\%$	1×10^{-14} (7.7σ)
Forward $W \rightarrow e\nu$ ($1.5 < \eta < 2.5$)	$(0.64 + 0.18 - 0.16)\%$	6×10^{-8} (5.3σ)
Total $W \rightarrow e\nu$	$(0.89 + 0.19 - 0.17)\%$	3×10^{-14} (7.5σ)
Total $Z \rightarrow e^+e^-$	$(1.44 + 0.61 - 0.52)\%$	5×10^{-6} (4.4σ)

TABLE III. Measured gap fractions and probabilities for non-diffractive W and Z boson events to fluctuate and mimic diffractive W and Z boson production.

We have thus far considered only non-diffractive W and Z boson events as the relevant background to diffractive production. We now consider contamination from events other than the desired $W \rightarrow e\nu$ and $Z \rightarrow ee$ states, drawing primarily on the work of Ref. [20].

The largest background to W boson production is from multijet events in which one jet is misidentified as an electron, while another is measured incorrectly, thereby providing large \cancel{E}_T . The fraction of fake $W \rightarrow e\nu$ events from multijet production was calculated [20] to be 0.046 ± 0.014 and 0.143 ± 0.043 of the total $W \rightarrow e\nu$ events for the central and forward electron samples, respectively. We use these fractions to determine the number of multijet events in our samples, and use measurements from Ref. [11] to obtain the number of diffractive events expected from this background. The results are shown in Table IV: for the central electron sample, a total of 0.88 diffractive events are expected from the 401 multijet background events. Given that there are 8724 events in the central electron W boson sample, with a measured diffractive fraction of $1.08 \pm_{0.17}^{0.19}\%$, we expect a total of $94 \pm_{15}^{17}$ diffractive events. Recalculating the central W boson gap fraction after subtracting the multijet background gives a slightly higher value of 1.11% (93/8323). We note that this 3% change is an upper limit, because multijet background in events with single interactions

would likely be smaller than in the inclusive W boson sample due to smaller fluctuations expected in $\#_T$. The forward sample gives a negligible correction, since the gap fraction from diffractive W boson signal and multijet background are nearly identical.

Sample	Total Events	Multijet Fraction	Multijet Events	Diffractive Dijet Fraction	Diffractive Multijet Events
central W	8724	0.046 ± 0.014	401	$0.22 \pm 0.05\%$	0.88
forward W	3898	0.143 ± 0.043	557	$0.65 \pm 0.04\%$	3.6

TABLE IV. The number of multijet background events in the diffractive W boson sample is calculated. Then, given the number of multijet events in the sample and the diffractive dijet rate, the number of diffractive events expected from these background events is calculated.

In addition to the multijet background, we consider background from misidentified Z boson events in which one electron is not detected. Again using methods from Ref. [20], we estimate 94 ± 24 Z boson events in the combined W boson sample, with 1.35 of these being diffractive W boson candidates. Subtracting this background would result in a less than 1% correction, in the opposite direction from the multijet correction, since the diffractive Z boson signal is larger than that of the diffractive W boson. Finally, the background level from $W \rightarrow \tau\nu$ is expected to be small (about 2%), and we would expect the same gap fraction from W bosons that decay to τ leptons as from the electron channel, therefore no correction is needed.

Combining all these background sources yields a total background to diffractive W boson production of at most 2%, which is insignificant compared to the total 20% uncertainty, and we therefore do not apply any correction. Similar considerations for the diffractive Z boson sample yield at most a 4% background correction factor, which is again not significant, and consequently not applied.

In this paper we have chosen to present the gap fraction, which is directly based on observable quantities. We thus avoid the reliance on potentially large model-dependent corrections. Therefore the measured gap fraction of $1.08 \pm_{0.17}^{0.19} \%$ for central electron W boson events cannot be directly compared to the CDF measurement of $(1.15 \pm 0.55)\%$ [16], which includes a correction factor derived from the POMPYT diffractive Monte Carlo [22] (based on the Ingelman-Schlein model) to attempt to account for how often a diffractive event does not yield a rapidity gap. They obtained a correction factor of 0.81 based on their Beam-Beam Counter (BBC) multiplicity, implying an uncorrected value of $(0.93 \pm 0.44)\%$, which is consistent with our measurement. However, this correction factor is quite different from that obtained by DØ and CDF using two-dimensional (luminosity counter and calorimeter multiplicity) methods subsequently adopted by both collaborations to extract rapidity gap signals. We obtain a correction factor of 0.21 ± 0.04 from our diffractive W boson Monte Carlo using a quark structure for the pomeron, which compares well with the quark-structure-based correction for our central jet measurement (0.18) [18] and the CDF

correction factor for their diffractive b -quark production (0.22) [7] and J/Ψ production (0.29) [8]. Since there is no consensus on the correct model for describing diffractive data at the Tevatron, we feel that using POMPYT to correct the data is not advisable, but it should be noted that our corrected W boson gap fraction would be 5.1% according to this model, while there would be no correction needed for non-pomeron models such as SCI.

Next, we calculate the ratio of the diffractive W and Z boson cross sections. In addition to intrinsic interest in this measurement, it is a potentially important input to the systematic uncertainty on the ratio R of the two cross sections [20]. We can write the diffractive cross section ratio R_D in terms of the gap fractions and the ratio R as follows:

$$R_D = \frac{W_D}{Z_D} = \left(\frac{W_D}{W} / \frac{Z_D}{Z} \right) \times R = 6.45 \pm_{2.64}^{3.06}, \quad (1.1)$$

where we have substituted the measured gap fractions W_D/W and Z_D/Z from this Letter, and the measured value $R = 10.43 \pm 0.15(stat) \pm 0.20(syst) \pm 0.10(NLO)$ [20], which takes into account acceptance differences between the W and Z boson samples (assumed to be similar for diffractive and non-diffractive events). This value of R_D is consistent with the ratio for non-diffractive production.

Finally, we measure the fractional momentum loss of the scattered proton ξ using the following equation [23]:

$$\xi \approx \frac{1}{\sqrt{s}} \sum_i E_{T_i} e^{\eta_i} \quad (1.2)$$

where E_{T_i} and η_i denote the transverse energy and pseudorapidity, respectively, of the observed particles. The η of the outgoing scattered proton or antiproton (and the rapidity gap) is defined to be positive. As discussed in Ref. [11], Eq. 1.2 is particularly sensitive to particles emitted in the well-measured central region near the rapidity gap, while particles lost down the beam pipe at negative η have negligible effect. Using a sample of POMPYT W boson events, where ξ can be determined from the momentum of the scattered proton, we have verified that Eq. 1.2 is valid independent of pomeron structure. A scale factor 1.5 ± 0.3 , derived by passing the Monte Carlo data through a full detector simulation, is used to convert ξ measured from all particles to that from just the electromagnetic energy depositions in the calorimeter [21]. Figure 5 shows the ξ distribution for the diffractive W boson candidate event sample with $n_{CAL} = n_{L\emptyset} = 0$. The mean ξ is 0.052 and most of the events have $\xi < 0.1$. Comparison of this ξ distribution obtained from calorimeter information with that from the measured proton using the upgraded DØ detector in Run II will give important insight into the nature of diffraction.

In conclusion, we have observed diffractive W boson production with greater than 7σ significance, shown that these diffractive W boson candidates have similar properties to non-diffractive ones, and measured the fraction of W boson events that are produced diffractively, in both the central and forward regions. We also have provided the first evidence for diffractive Z boson production. The extracted gap fractions have no model-dependent corrections, and are typically about 1%, far below expectations for a quark-dominated pomeron. We have obtained a ratio of diffractive W and Z boson cross sections consistent with the ratio for non-diffractive production.

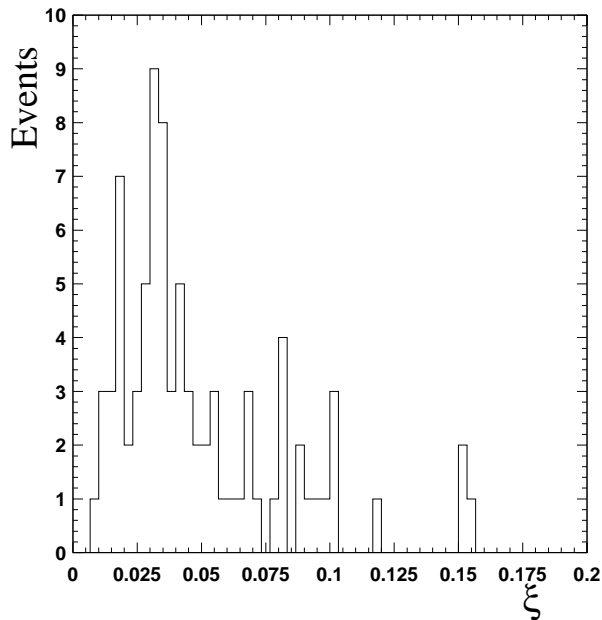


FIG. 5. The ξ distribution for the combined central and forward electron W boson data with $n_{\text{CAL}} = n_{\text{LO}} = 0$, extracted from calorimeter information as described in the text.

We have also measured the fractional momentum lost by the scattered proton and found that typically less than 10% of the proton momentum takes part in the hard scattering, with an average of about 5%.

We thank the staffs at Fermilab and collaborating institutions, and acknowledge support from the Department of Energy and National Science Foundation (USA), Commissariat à L'Energie Atomique and CNRS/Institut National de Physique Nucléaire et de Physique des Particules (France), Ministry for Science and Technology and Ministry for Atomic Energy (Russia), CAPES, CNPq and FAPERJ (Brazil), Departments of Atomic Energy and Science and Education (India), Colciencias (Colombia), CONACyT (Mexico), Ministry of Education and KOSEF (Korea), CONICET and UBACyT (Argentina), The Foundation for Fundamental Research on Matter (The Netherlands), PPARC (United Kingdom), Ministry of Education (Czech Republic), A.P. Sloan Foundation, and the Research Corporation.

REFERENCES

* Visitor from University of Zurich, Zurich, Switzerland.

† Visitor from Institute of Nuclear Physics, Krakow, Poland.

- [1] P.D.B. Collins, *An Introduction to Regge Theory and High Energy Physics*, Cambridge University Press, Cambridge (1977).
- [2] G. Ingelman and P. Schlein, Phys. Lett. B **152**, 256 (1985).
- [3] R. Bonino *et al.* (UA8 Collaboration), Phys. Lett. B **211**, 239 (1988); A. Brandt *et al.* (UA8 Collaboration), Phys. Lett. B **297**, 417 (1992).
- [4] F. Abe *et al.* (CDF Collaboration), Phys. Rev. Lett. **79**, 2636 (1997).
- [5] J. Breitweg *et al.* (ZEUS Collaboration), Eur. Phys. J. **C5**, 41 (1998) and references therein.
- [6] C. Adloff *et al.* (H1 Collaboration), Eur. Phys. J. **C6**, 421 (1999).
- [7] T. Affolder *et al.* (CDF Collaboration), Phys. Rev. Lett. **84**, 232 (2000).
- [8] T. Affolder *et al.* (CDF Collaboration), Phys. Rev. Lett. **87**, 241802 (2001).
- [9] L. Alvero, J.C. Collins, J. Terron and J. Whitmore, Phys. Rev. D **59**, 74022 (1999).
- [10] T. Affolder *et al.* (CDF Collaboration), Phys. Rev. Lett. **84**, 5043 (2000).
- [11] B. Abbott *et al.* (DØ Collaboration), Phys. Lett. B **531**, 52 (2002).
- [12] V. A. Khoze, A. D. Martin, and M.G. Ryskin, Phys. Lett. B **502**, 87 (2001) and references therein.
- [13] A. Edin, G. Ingelman, and J. Rathsmann, J. Phys. G **22**, 943 (1996).
- [14] P. Bruni and G. Ingelman, Phys. Lett. B **311**, 317 (1993).
- [15] N. Timneanu, R. Enberg, and G. Ingelman, hep-ph/0111210, 2001 (unpublished).
- [16] F. Abe *et al.* (CDF Collaboration), Phys. Rev. Lett. **78**, 2698 (1997).
- [17] S. Abachi *et al.* (DØ Collaboration), Nucl. Instrum. Methods in Phys. Res. A **338**, 185 (1994).
- [18] K. Mauritz, Ph.D. Dissertation, Iowa State University, 1999 (unpublished).
- [19] B. Abbott *et al.* (DØ Collaboration), Phys. Rev. D **58**, 092003 (1998).
- [20] B. Abbott *et al.* (DØ Collaboration), Phys. Rev. D **61**, 072001 (2000).
- [21] L. Coney, Ph. D. Thesis: Diffractive W and Z Boson Production in $\bar{p}p$ Collisions at $\sqrt{s} = 1800$ GeV, 2000 (unpublished).
- [22] P. Bruni and G. Ingelman, DESY 93-187, 1993 (unpublished). We used a modified version of POMPYT 2.6.
- [23] J. Collins, hep-ph/9705393, 1997 (unpublished).